Electronic Supplementary Material (ESI) for ChemComm.
This journal is © The Royal Society of Chemistry 2019

Supporting Information

Single Sb sites for efficient electrochemical CO_2 reduction

Mingwen Jia,[a] Song Hong,[b] Tai-Sing Wu,[c] Xin Li,[a] Yun-Liang Soo[c] and Zhenyu Sun[a,*]

[a] State Key Laboratory of Organic–Inorganic Composites, College of Chemical Engineering, Beijing University of Chemical Technology, Beijing 100029, P. R. China. E-mail: sunzy@mail.buct.edu.cn

[b] Analysis Technology R&D Center, Beijing University of Chemical Technology, P. R. China

[c] Department of Physics, National Tsing Hua University, Hsinchu, 30013, Taiwan

Experimental section

Chemicals and reagents

All chemicals used in this work were of analytical grade and used without further treatments. Carbon black (Vulcan XC-72) was purchased from Fuel Cell Store. Urea and antimony trichloride were obtained from Aladdin. Ethanol, sulfuric acid, phosphoric acid, and nitric acid were obtained from Beijing Chemical Reagent Company. Nafion solution (5.0 wt%) was purchased from Sigma-Aldrich and Nafion membranes were provided by Alfa Aesar. Deionized water was used in all experiments.

Catalyst preparation

Synthesis of Sb_NC

In a typical procedure to synthesize N-doped carbon supported Sb SACs (denoted as Sb_NC), 100 mg of carbon black (Vulcan XC-72) was first activated by dispersing in 20 mL of 9 M nitric acid solution followed by refluxing at 90 ºC for 3 h. After washing and drying, this activated carbon black mixed with 1000 mg of urea were added into 15 mL of antimony chloride ethanol solution (containing 5 mg of Sb^{3+}). After ultrasonication for 30 min, a homogeneous dispersion was achieved, which was dried at 60 °C to evaporate the solvent. The obtained solid was then ground into powder and pyrolyzed at 800 ºC for 2 h under an argon atmosphere.

The same procedure has been applied for the preparation of Sb_C without urea.

Characterization

XPS experiments were carried out using Thermo Scientific ESCALAB 250Xi instrument. The instrument was equipped with an electron flood and scanning ion gun. All spectra were calibrated to the C 1s binding energy at 284.8 eV. X-ray powder diffraction (XRD) was performed with a D/MAX-RC diffractometer operated at 30 kV and 100 mA with Cu Kα radiation. High-angle annular dark field scanning TEM (HAADF-STEM) was conducted using a JEOL ARM200 microscope with 200 kV accelerating voltage. STEM samples were prepared by depositing a droplet of suspension onto a Cu grid coated with a Lacey Carbon film. Nitrogen adsorption/desorption measurements at 77 K were performed on a Micromeritics ASAP2460 to obtain pore properties such as the specific surface area, total pore volume, and pore size distribution. The sample was degassed at 200 °C for 10 h. Raman spectra were collected with a Renishaw in Via Raman microscope with a He/Ne Laser excitation at 532 nm (2.33 eV).

Cathode preparation

Typically, 10 mg of catalyst was dispersed in 2 mL of a mixture containing isopropanol, deionized water, and 5 wt% Nafion solution with a volume ratio of 100: 100: 1 under ultrasonication for 30 min to form a homogeneous ink. 200 μL of the dispersion was then loaded onto a carbon paper electrode with an area of 1 cm × 1 cm and dried under ambient conditions. For linear sweep voltammograms in Ar- or CO_2-saturated 0.1 M $KHCO_3$ solution, 6 mg of a catalyst was dispersed in the mixture of 600 μL of ethanol, 600 μL of deionized water, and 600 μL of Nafion solution (1 wt%). Then the mixture was ultrasonicated for 30 min to form a homogeneous ink. 7.95 μL of the dispersion was then loaded onto glassy carbon electrode and dried under ambient conditions.

Electrochemical measurements

Controlled potential electrolysis of CO_2 was tested in an H-cell system (Fig. S5), which was separated by a Nafion 117 membrane. Before ECR tests, the Nafion membrane was pre-treated subsequently by heating in 5% H_2O_2 aqueous solution and 0.5 M H_2SO_4 at 80 °C for 1 h. Then the Nafion membrane was immersed in deionized water under ambient conditions for 30 min and then washed with deionized water. Toray Carbon fiber paper with a size of 1 cm × 1 cm was used as working electrode. Pt wire and Ag/AgCl electrodes were used as counter electrode and reference electrode, respectively. The potentials were controlled by an electrochemical working station (CHI 760E, Shanghai CH Instruments Co., China). All potentials in this study were measured against the Ag/AgCl reference electrode (in 3.5 M KCl solution) and converted to the RHE reference scale by

$$E\ (vs.\ \mathrm{RHE}) = E\ (vs.\ \mathrm{Ag/AgCl}) + 0.21\ \mathrm{V} + 0.0591 \times \mathrm{pH} \qquad \text{(Eq. S1)}$$

Electrocatalytic CO_2 reduction was conducted in CO_2-saturated 0.1 M $KHCO_3$ solution at room temperature and atmospheric pressure. CO_2 was purged into the $KHCO_3$ solution for at least 30 min to remove residual air in the reservoir, then controlled potential electrolysis was performed at each potential for 60 min.

Gaseous products from the cell were analyzed using an Agilent 7890B GC system. Two thermal conductivity detectors and a flame ionization detector were applied to analyze and differentiate the injected samples. To characterize the gas product, 20 mL of the gas products in the dead volume of a gas bag (~1 L) was injected into the GC under identical experimental conditions (e.g., pressure, temperature, and time) using a sample lock syringe. CO and H_2 peaks were detected at 11.4 and 3.7 min, respectively. The liquid product was analyzed in DMSO-d6 with tetramethylsilane (TMS) as an internal standard by ^1H nuclear magnetic resonance (NMR) (Bruker Avance III 400 HD spectrometer). No liquid products including formate were detectable by ^1H NMR at -0.9 V (*vs*. RHE) in CO_2-saturated 0.5 M $KHCO_3$ solution (Fig. S6). This suggests that CO and H_2 were the main products as detected by GC.

Faradaic efficiency (FE) measurements

The FE values of catalysts were calculated using $FE = \frac{Z * n * F}{Q_{total}}$ (Eq. S2) where *Z* is the number of electrons transferred (Z = 2 for CO and H_2 production), *n* the number of moles for a given product, *F* Faraday's constant (96 485 C mol^{-1}), Q_{total} all the charge passed throughout the electrolysis process (measured by calculating the curve area of current density *vs*. time plot). CO and H_2 mole fractions of injected samples were calculated based on GC calibration curve.

Partial current density determination

Partial current density for CO or H_2 can be obtained by multiplying corresponding FE by the total current density (*J*):

$$J_{\text{CO or H}_2} = J \times \text{FE}_{\text{CO or H}_2} \qquad \text{(Eq. S3)}$$

Number of active sites and turnover frequency (TOF) measurements

The TOF for CO formation was calculated as follows:

$$TOF = \frac{J_{CO} \times S/ZF}{m_{cat.} \times \omega/M_{Ni}} \times 3600 \qquad \text{(Eq. S4)}$$

where J_{CO} is CO partial current (A cm^{-2}), *S* is the geometric surface area of working electrode (cm^2), *Z* is the number of electrons transferred ($Z = 2$ for CO formation), *F* is Faraday’s constant (96 485 C mol^{-1}), $m_{cat.}$ is catalyst mass in the electrode (g), ω is Sb loading in the catalyst, and M_{Sb} is atomic mass of Sb (121.8 g mol^{-1}).

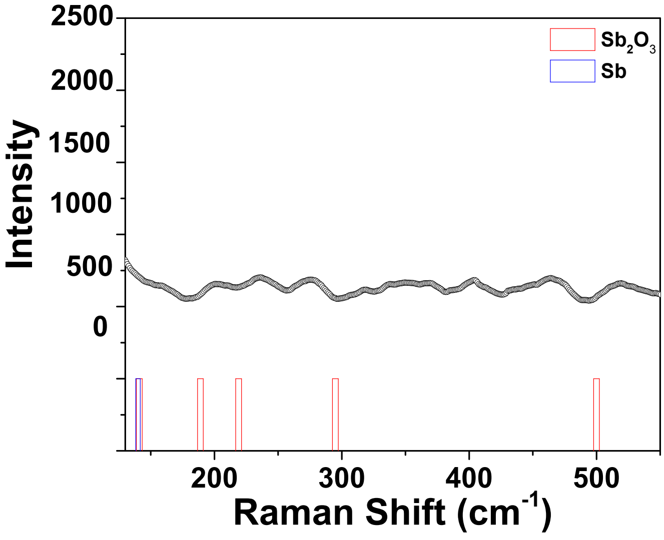

Fig. S1 Raman spectrum of Sb_NC. Major typical Raman peaks from Sb and Sb_2O_3 are added at the bottom for reference.

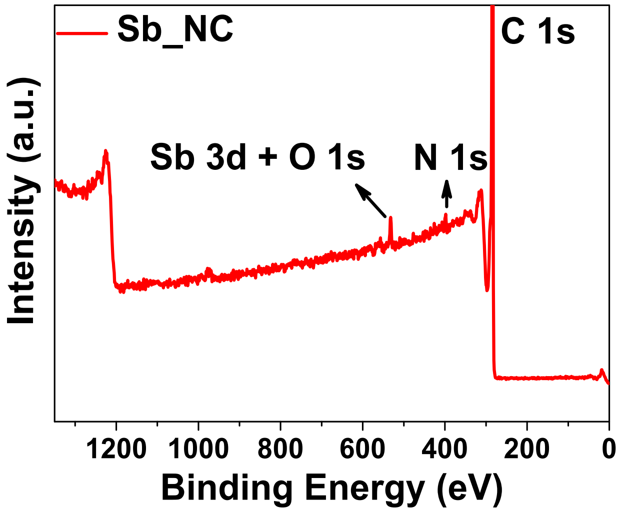

Fig. S2 Wide-survey XPS spectrum of Sb_NC.

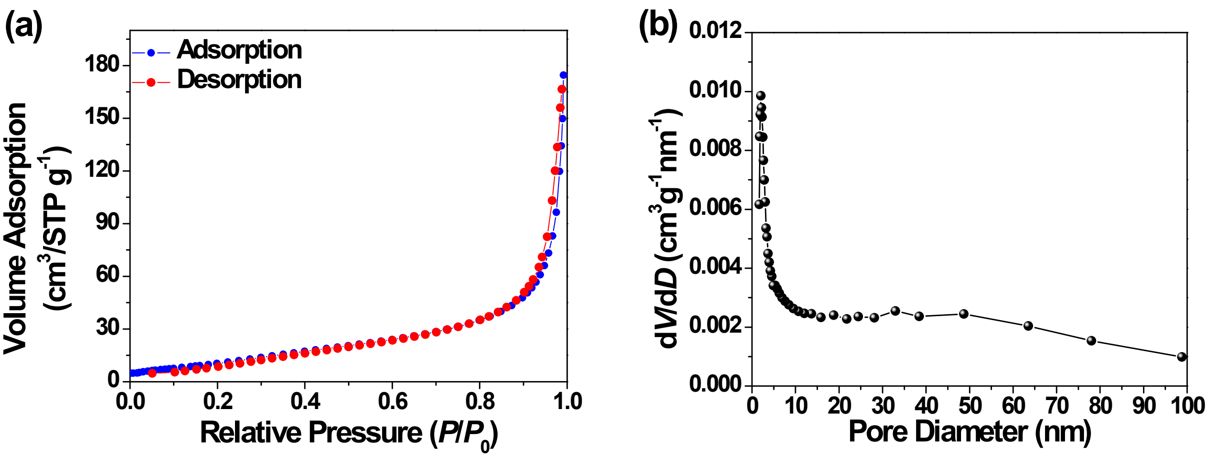

Fig. S3 (a) N_2 adsorption-desorption isotherms of Sb_NC. (b) Plot of pore size distribution of Sb_NC calculated from the desorption branch of the isotherms.

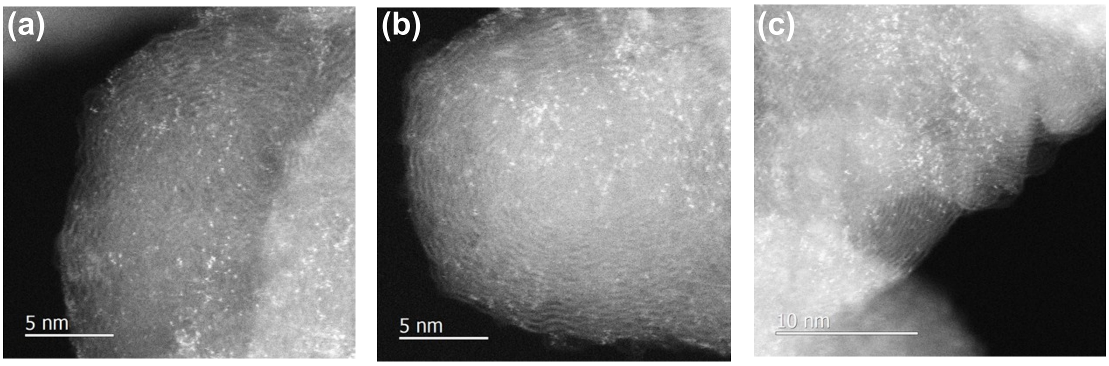

Fig. S4 (a)-(c) HAADF-STEM images of Sb_NC over different regions.

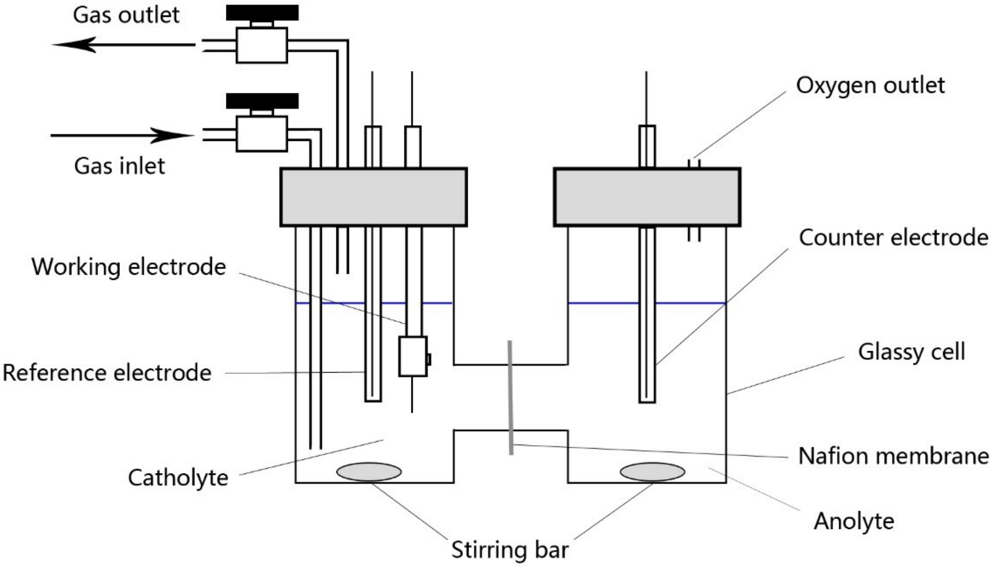

Fig. S5 Illustration of an H-type cell for CO_2 electrolysis.

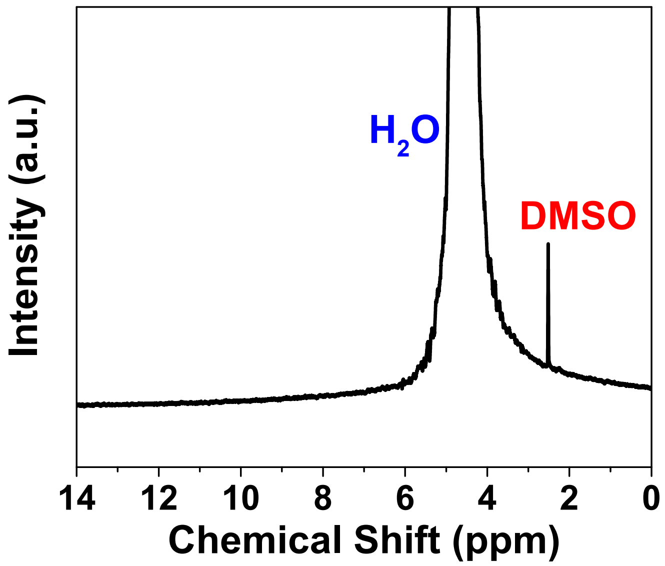

Fig. S6 ^{1}H NMR plot of liquid electrolyte after 1 h of CO_2 electrolysis at -0.9 V *vs*. RHE.

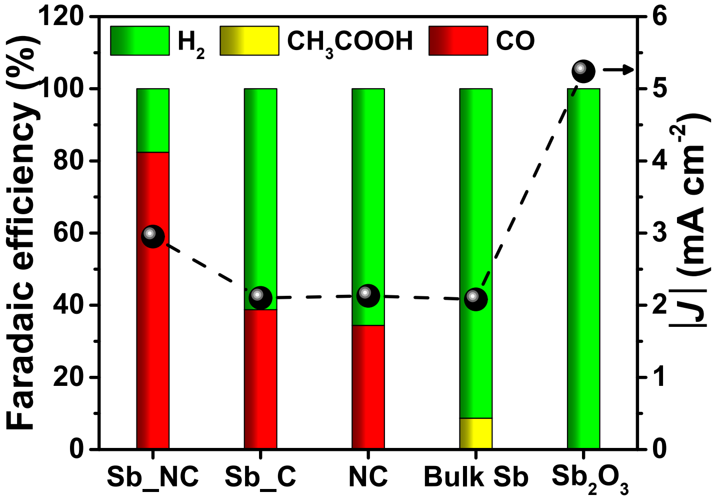

Fig. S7 Faradaic efficiencies (bar) and current densities (ball) of Sb_NC, Sb_C, NC, bulk Sb, and Sb_2O_3 at -0.9 V (*vs*. RHE).

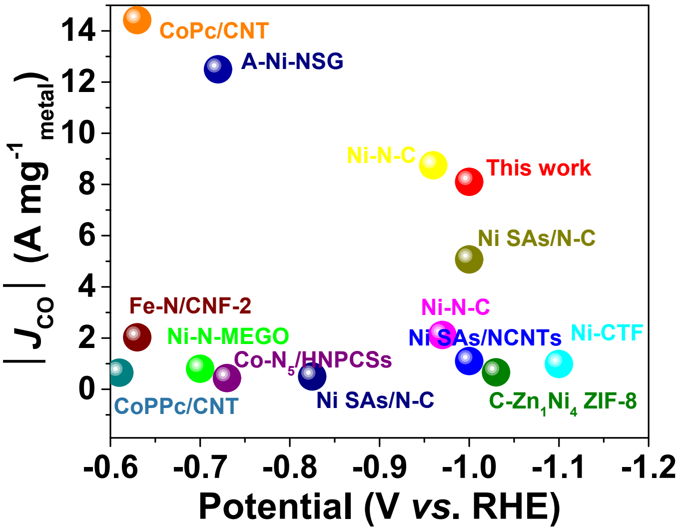

Fig. S8 CO partial current density of Sb_NC compared with those of other reported single atom catalysts with details listed in Table S1.

Table S1. Summary for the reported single metal atom-based ECR electrocatalysts.

Catalyst	Potential/ V *vs*. RHE	CO partial current density/ mA cm^{-2}	Catalyst mass/g cm^{-2}	Metal content	Metal mass activity/mA mg^{-1}	TOF	Ref.
Sb_NC	-0.9	2.43	10^{-3}	0.03 wt%	8100	11577	This work
Ni-N-MEGO	-0.7	26.8	$5*10^{-4}$	6.7 wt%	800	875.92	1
Ni SAs/NCNTs	-1.0	55.38	$8*10^{-4}$	6.63 wt%	1098	1176	2
Ni-CTF	-1.1	2.45	$3*10^{-4}$	0.83 wt%	983	1077.3	3
Ni-N-C	-0.97	18	$3*10^{-4}$	2.83 wt%	2120	2321.3	4
Ni-N-C	-0.96	10.5	$5*10^{-4}$	0.24 wt%	8750	9580.3	5
Ni-N-Gr	-0.8	N/A	$3*10^{-4}$	2.2 wt%	N/A	4600	6

Ni SAs/N-C	-1.0	7.37	$1*10^{-4}$	1.53 wt%	5070	5273	7
Ni-N-C	-0.825	12.92	$7.6*10^{-4}$	0.7 at.% ≈ 3.42 wt%	497	544	8
Co–N$_5$/HNPCSs	-0.73	4.5	$3*10^{-4}$	3.44 wt%	436	480.2	9
Fe-N/CNF-2	-0.63 V	6.69	10^{-3}	0.33 wt%	2027	7114	10
C-Zn$_1$Ni$_4$ ZIF-8	-1.03	71.5	$2*10^{-3}$	5.44 wt%	657.2	10087	11
CoPPc/CNT	-0.61	16.8	10^{-3}	2.6 wt%	646	4896	12
A-Ni-NSG	-0.72	35	10^{-4}	2.8 wt%	12500	14800	13
CoPc/CNT	-0.63	15.0	$4*10^{-4}$	0.26 wt%	14423	14760	14

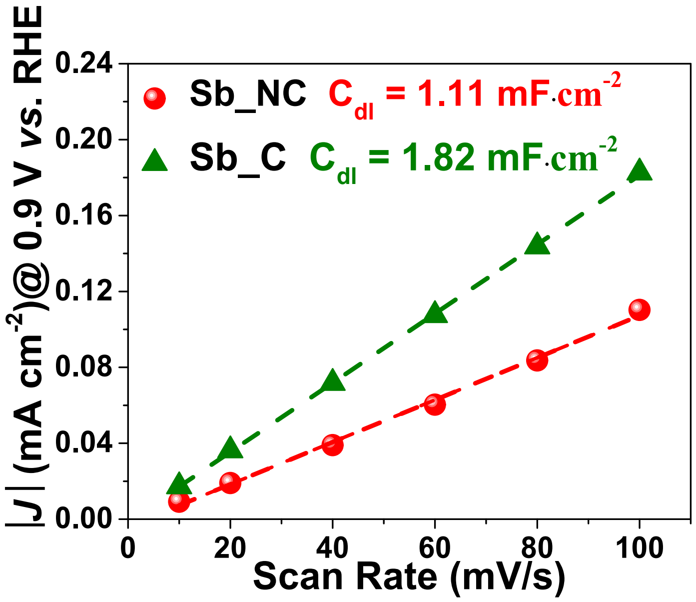

Fig. S9 Charging current density differences plotted against scan rates.

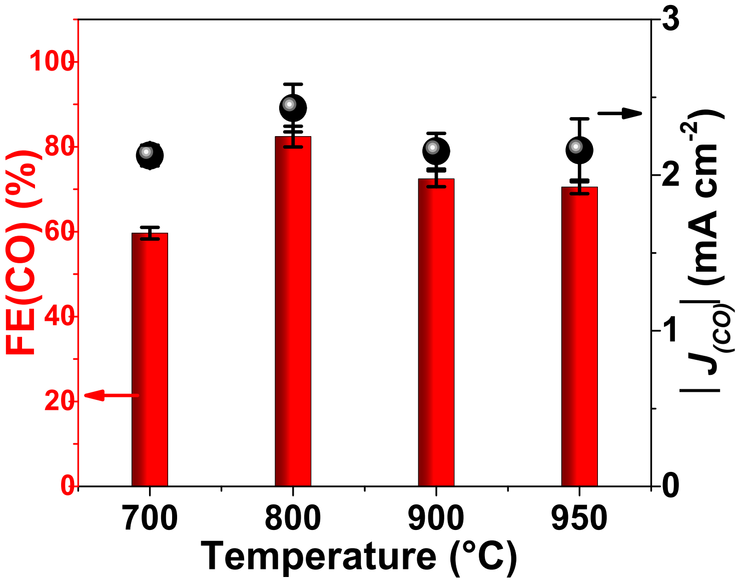

Fig. S10 CO FEs and partial current densities at -0.9 V (*vs*. RHE) of Sb_NC obtained at 700, 800, 900, and 950 ºC in Ar for 2 h.

References

[1] Y. Cheng, S. Y. Zhao, H. B. Li, S. He, J.-P. Veder, B. Johannessen, J. P. Xiao, S. F. Lu, J. Pan, M. F. Chisholm, S. Z. Yang, C. Liu, J. G. Chen and S. P. Jiang, *Appl. Catal., B*, 2019, **243**, 294-303.

[2] P. L. Lu, Y. J. Yang, J. N. Yao, M. Wang, S. Dipazir, M. L. Yuan, J. X. Zhang, X. Wang, Z. J. Xie and G. J. Zhang, *Appl. Catal., B*, 2019, **241**, 113-119.

[3] P. P. Su, K. Iwase, T. Harada, K. Kamiya and S. Nakanishi, *Chem. Sci.*, 2018, **9**, 3941-3947.

[4] F. P. Pan, W. Deng, C. Justiniano and Y. Li, *Appl. Catal., B*, 2018, **226**, 463-472.

[5] X. M. Hu, H. H. Hval, E. T. Bjerglund, K. J. Dalgaard, M. R. Madsen, M.-M. Pohl, E. Welter, P. Lamagni, K. B. Buhl, M. Bremholm, M. Beller, S. U. Pedersen, T. Skrydstrup and K. Daasbjerg, *ACS Catal.*, 2018, **8**, 6255-6264.

[6] P. P. Su, K. Iwase, S. Nakanishi, K. Hashimoto and K. Kamiya, *Small*, 2016, **12**, 6083-6089.

[7] C. M. Zhao, X. Y. Dai, T. Yao, W. X. Chen, X. Q. Wang, J. Wang, J. Yang, S. Q. Wei, Y. Wu and Y. D. Li, *J. Am. Chem. Soc.*, 2017, **139**, 8078-8081.

[8] W. Ju, A. Bagger, G. P. Hao, A. S. Varela, I. Sinev, V. Bon, B. Roldan Cuenya, S. Kaskel, J. Rossmeisl and P. Strasser, *Nat. Commun.*, 2017, **8**, 944-953.

[9] Y. Pan, R. Lin, Y. Chen, S. Liu, W. Zhu, X. Cao, W. Chen, K. Wu, W.-C. Cheong, Y. Wang, L. Zheng, J. Luo, Y. Lin, Y. Liu, C. Liu, J. Li, Q. Lu, X. Chen, D. Wang, Q. Peng, C. Chen and Y. Li, *J. Am. Chem. Soc.*, 2018, **140**, 4218-4221.

[10] Q. Cheng, K. Mao, L. Ma, L. Yang, L. Zou, Z. Zou, Z. Hu and H. Yang, *ACS Energy Lett.*, 2018, **3**, 1205-1211.

[11] C. C. Yan, H. B. Li, Y. F. Ye, H. H. Wu, F. Cai, R. Si, J. P. Xiao, S. Miao, S. H. Xie, F. Yang, Y. S. Li, G. X. Wang and X. H. Bao, *Energy Environ. Sci.*, 2018, **11**, 1204-1210.

[12] N. Han, Y. Wang, L. Ma, J. G. Wen, J. Li, H. C. Zheng, K. Q. Nie, X. X. Wang, F. P. Zhao, Y. F. Li, J. Fan, J. Zhong, T. P. Wu, D. J. Miller, J. Lu, S. T. Lee and Y. G. Li, *Chem*, 2017, **3**, 652–664.

[13] H. B. Yang, S. F. Hung, S. Liu, K. D. Yuan, S. Miao, L. P. Zhang, X. Huang, H. Y. Wang, W. Z. Cai, R. Chen, J. J. Gao, X. F. Yang, W. Chen, Y. Q. Huang, H. M. Chen, C. M. Li, T. Zhang and B. Liu, *Nat. Energy*, 2018, **3**, 140-147.

[14] X. Zhang, Z, S. Wu, X. Zhang, L. W. Li, Y. Y. Li, H. M. Xu, X. X. Li, X. L. Yu, Z. S. Zhang, Y. Y. Liang and H. L. Wang, *Nat. Commun.,* 2017, **8**, 14675-14683